

# The Multichromophore Approach: Prolonged Room-Temperature Luminescence Lifetimes in Ru<sup>II</sup> Complexes Based on Tridentate Polypyridine Ligands

Jianhua Wang,<sup>[a]</sup> Yuan-Qing Fang,<sup>[a, b]</sup> Laurence Bourget-Merle,<sup>[a]</sup> Matthew I. J. Polson,<sup>[a, c]</sup> Garry S. Hanan,<sup>\*[a]</sup> Alberto Juris,<sup>\*[d]</sup> Frédérique Loiseau,<sup>[e]</sup> and Sebastiano Campagna<sup>\*[e]</sup>

**Abstract:** A new family of ruthenium(II) complexes with multichromophoric properties was prepared based on a “chemistry-on-the-complex” synthetic approach. The new compounds are based on tridentate chelating sites (tpy-type ligands, tpy = 2,2':6',2''-terpyridine) and most of them carry appended anthryl chromophores. Complexes **2a** and **2b** were synthesized through the Pd-catalyzed Suzuki coupling reaction between 9-anthrylboronic acid and the chloro ligands on the precursor species **1a** and **1b**, respectively. The mono-coupling product **2c** was also synthesized as the starting complex for a di-metallic complex under optimized Suzuki coupling conditions. The palladium(0)-catalyzed homocoupling reaction on complexes **1a** and **2c** led to di-metallic Ru<sup>II</sup> species **2d** and **2e**, respectively. The solid structures of complexes **2a** and **2b** were characterized by X-ray diffraction. The absorption

spectra, redox behavior, luminescence properties (both at room temperature and at 77 K), and transient absorption spectra and decays of **2a–e** were investigated. The absorption spectra of all new species are dominated by ligand-centered (LC) bands in the UV region and metal-to-ligand charge-transfer (MLCT) bands in the visible region. The new compounds undergo reversible metal-centered oxidation processes and several ligand-centered reduction processes, which have been assigned to specific sites. The complexes exhibit luminescence both at room temperature in fluid solution and at 77 K in rigid matrices; the emission was attributed to <sup>3</sup>MLCT states at room temperature

and to the lowest-lying anthracene triplet (<sup>3</sup>An) at low temperature, except for **2c**, which does not contain any anthryl chromophore and whose low temperature emission is also of MLCT origin. The luminescence lifetimes of complexes **2a–d** showed that multichromophoric behavior occurs in these species, allowing the luminescence lifetime of the Ru<sup>II</sup>-based chromophores to be prolonged to the microsecond timescale, with the anthryl groups behaving as energy-storage elements for the repopulation of the <sup>3</sup>MLCT state. Nanosecond transient-absorption spectroscopy confirmed the equilibration process between the triplet MLCT and An levels at room temperature. Thermodynamic and kinetic factors governing the equilibration time and the lifetime of the equilibrated excited state are discussed.

**Keywords:** C–C coupling • excited-state lifetimes • luminescence • N ligands • ruthenium complexes • tridentate ligands


[a] J. Wang, Y.-Q. Fang, Dr. L. Bourget-Merle, Dr. M. I. J. Polson, Prof. Dr. G. S. Hanan  
Département de Chimie, Université de Montréal  
2900 Edouard Montpetit, Montréal, QC, H3T 1J4 (Canada)  
Fax: (+1) 514-343-2468  
E-mail: garry.hanan@umontreal.ca

[b] Y.-Q. Fang  
Present address: Department of Chemistry, University of Toronto  
Toronto, Ontario (Canada)

[c] Dr. M. I. J. Polson  
Present address: Department of Chemistry, Canterbury University  
Christchurch (New Zealand)

[d] Prof. Dr. A. Juris  
Dipartimento di Chimica “G. Ciamician”, Università di Bologna  
Via F. Selmi 2, 40126 Bologna (Italy)  
Fax: (+39) 051-209-9456  
E-mail: alberto.juris@unibo.it

[e] Dr. F. Loiseau, Prof. Dr. S. Campagna  
Dipartimento di Chimica Inorganica  
Chimica Analitica e Chimica Fisica, Università di Messina  
Via Sperone 31, 98166 Messina (Italy)  
Fax: (+39) 090-393-756  
E-mail: campagna@unime.it

 Supporting information for this article is available on the WWW under <http://www.chemeurj.org/> or from the author.

## Introduction

Luminescent multicomponent systems (LMS) are important targets in supramolecular chemistry as they play important roles in fields connected to solar energy conversion and storage of light and/or electronic information at the molecular level.<sup>[1]</sup> Although their synthesis normally requires elaborate procedures, recent advances have facilitated the synthesis of an important class of LMS based on ruthenium(II) polypyridine complexes.<sup>[1a]</sup> For example, multinuclear complexes having dendritic shape and containing up to 22 Ru<sup>II</sup> centers were prepared by a series of protection/deprotection sequences.<sup>[2]</sup> These light-harvesting complexes were shown to channel excitation energy based on the substitution pattern of the dendrimers.<sup>[3]</sup> More recently, new binding sites were created in metal complexes by organometallic coupling reactions catalyzed by nickel(0)<sup>[4]</sup> and palladium(0).<sup>[5]</sup> These new building blocks could be exploited for further metal-ion coordination or as ion sensors.<sup>[6]</sup>

[Ru(bpy)<sub>3</sub>]<sup>2+</sup>-type (bpy = 2,2'-bipyridine) moieties have been widely used for building polymetallic complexes as they display a combination of chemical stability, and suitable redox and photophysical properties.<sup>[7]</sup> However, [Ru(tpy)<sub>2</sub>]<sup>2+</sup> (tpy = 2,2':6',2''-terpyridine) complexes have stereochemical advantages if incorporated into multinuclear supramolecular arrays, due to the absence of  $\Delta$  and  $\Lambda$  enantiomers that exist in *D*<sub>3</sub>-symmetrical [Ru(bpy)<sub>3</sub>]<sup>2+</sup> complexes.<sup>[8]</sup> Unfortunately, [Ru(tpy)<sub>2</sub>]<sup>2+</sup> complexes are practically nonluminescent at room temperature because of their short room-temperature excited-state lifetime (<0.25 ns).<sup>[8m]</sup> With such a short excited-state lifetime, energy transfer from the triplet metal-to-ligand charge-transfer (<sup>3</sup>MLCT) state of the ruthenium complexes to other suitable acceptor molecules is difficult to study and to apply. Prolonging the room-temperature excited-state lifetimes of [Ru(tpy)<sub>2</sub>]<sup>2+</sup> complexes is still a major challenge, and consequently, the chemistry of [Ru(tpy)<sub>2</sub>]<sup>2+</sup> complexes is much less developed than that of [Ru(bpy)<sub>3</sub>]<sup>2+</sup>.

Several synthetic strategies have been employed recently to prolong the room-temperature excited-state lifetime of ruthenium complexes with tridentate polypyridyl ligands.<sup>[8q]</sup> These include the use of 1) electron-deficient ligands,<sup>[9]</sup> 2) strong electron-donating ligands,<sup>[8m,n]</sup> 3) electron-withdrawing and/or donor substituents on terpyridine,<sup>[8o,p]</sup> and 4) ligands with extended acceptor orbitals.<sup>[10]</sup> The first three strategies increase the energy gap between the <sup>3</sup>MLCT and <sup>3</sup>MC excited states, thereby minimizing the thermally-activated surface crossing to the MC state, which is mainly responsible for radiationless decay. The last strategy is based on modification of the Frank–Condon factors for direct non-radiative decay from the MLCT state to the ground state. Quite recently, a further approach to increase the luminescence lifetime of metal polypyridine complexes has emerged: the combination of metal complexes and organic chromophores that have triplet excited states at similar energies.<sup>[11]</sup> For species built up according to this latter approach, the prolonged excited-state lifetimes are attributed to the energy equilibrium between <sup>3</sup>MLCT and triplet states

of the secondary chromophores, which serve as energy-storage elements in the LMS.

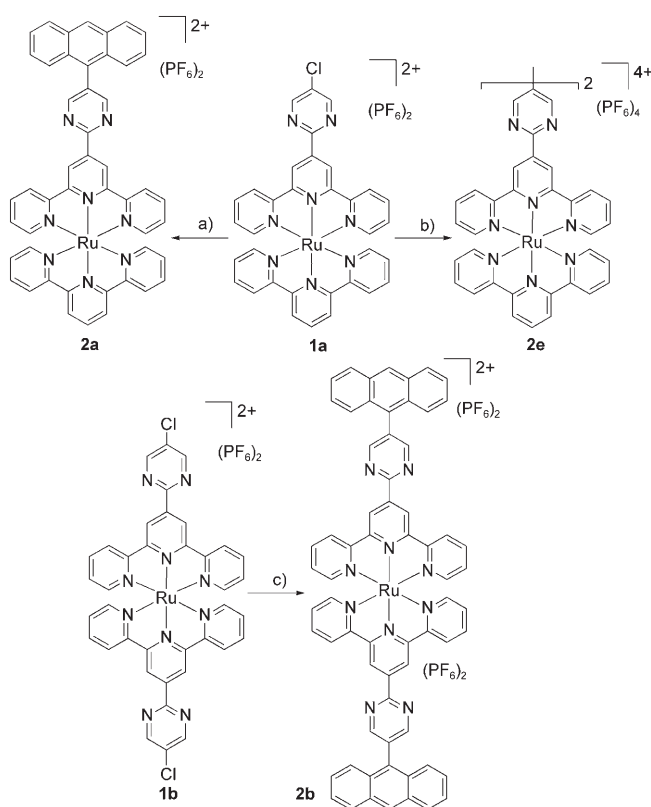
An example of the approach based on ligands with extended acceptor to prolong room-temperature excited-state lifetime of [Ru(tpy)<sub>2</sub>]<sup>2+</sup>-based complexes was obtained by introducing a coplanar pyrimidyl (pm) substituent on the tpy ligands. This resulted simultaneously in increased electron delocalization and enlargement of the <sup>3</sup>MLCT–<sup>3</sup>MC energy gap.<sup>[10d]</sup> Through this approach the room-temperature excited-state lifetime of [Ru(tpy-pm-R)<sub>2</sub>]<sup>2+</sup> (tpy-pm-R = 4'-(5-substituted-2-pyrimidyl)-2,2':6',2''-terpyridine) complexes can be prolonged up to 200 ns. Following these encouraging results, [Ru(tpy-pm-R)<sub>2</sub>]<sup>2+</sup> complexes based on the fusion of two approaches were prepared, that is, the coupling of ligands with extended  $\pi^*$  orbitals and an organic chromophore with a triplet-state energy level similar to the <sup>3</sup>MLCT state of the metal complex. Actually, the energy level of the <sup>3</sup>MLCT emitting state of [Ru(tpy-pm-R)<sub>2</sub>]<sup>2+</sup> complexes (between 1.83 and 1.87 eV with various 5-substituents on pm) can be tuned to the energy level of the nonemissive, longer-lived triplet state of an anthracene subunit (<sup>3</sup>An, *E*<sup>00</sup> about 1.85 eV),<sup>[12]</sup> which acts as the storage element in the bichromophore approach.

Herein we present our synthetic approach to incorporate anthracene subunits into [Ru(tpy-pm-R)<sub>2</sub>]<sup>2+</sup>-based complexes and the photophysical properties of these newly synthesized Ru<sup>II</sup> multichromophore species. Preliminary results on two complexes of the reported series (**2a** and **2b**) have been communicated previously.<sup>[13]</sup>

## Results and Discussion

**Synthesis:** Complexes **2a** and **2b** were synthesized by using the “chemistry-on-the-complex” methodology, in which the 4'-(5-(9-anthryl)pyrimid-2-yl)-2,2':6',2''-terpyridine (an-pm-tpy) ligands were synthesized while directly attached to the metal ion. This approach is particularly powerful if used in conjugation with organometallic catalysts to form carbon–carbon bonds. Previous work has shown that the chloro substituent in the 5-position of a pyrimidine group is relatively inert to Stille coupling reactions because it is *meta* to both nitrogen atoms.<sup>[14]</sup> However, the ruthenium cations in **1a** and **1b** effectively activate the 5-chloro group on the conjugated pyrimidine ring by an inductive effect.<sup>[15]</sup> Thus, ruthenium complexes **1a** and **1b** were allowed to react with 9-anthryl boronic acid<sup>[16]</sup> under Suzuki coupling conditions at elevated temperatures to afford complexes **2a** and **2b**, respectively (Scheme 1).<sup>[17]</sup>

The synthesis of the heteroleptic complex, [(Cl-pm-tpy)-Ru(tpy-pm-an)]<sub>2</sub>[PF<sub>6</sub>]<sub>2</sub> (**2c**), was initially attempted by using the standard approach used to construct 5-substituted pyrimidyl groups in the R-pm-tpy ligands. We envisioned the formation of the an-pm-tpy ligand through a pyrimidine-forming condensation reaction between 2-(9-anthryl)-1,3-bis(dimethylamino)trimethinium hexafluorophosphate and 2,2':6',2''-terpyrid-4'-ylamidine hydrochloride. However,

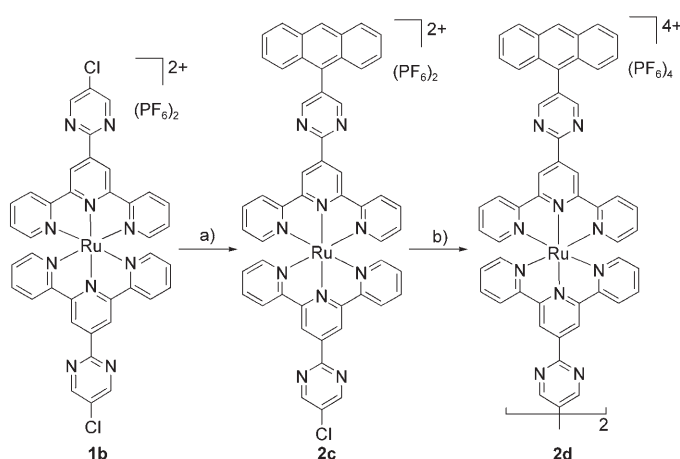


Scheme 1. Synthesis of complexes **2a**, **2b**, and **2e** by palladium-catalyzed reactions: a) excess 9-anthryl boronic acid, [PdCl<sub>2</sub>(PPh<sub>3</sub>)<sub>2</sub>], K<sub>2</sub>CO<sub>3</sub>, DMF, 110 °C, 12 h, yield: 85 %; b) 1.0 equiv **1a**, 15 mol % [Pd(OAc)<sub>2</sub>], 30 mol % *t*Bu<sub>2</sub>P(biph), 2.0 equiv K<sub>2</sub>CO<sub>3</sub>, DMF, 110 °C, 24 h, yield: 75 %; c) excess 9-anthryl boronic acid, [PdCl<sub>2</sub>(PPh<sub>3</sub>)<sub>2</sub>], K<sub>2</sub>CO<sub>3</sub>, DMF, 140 °C, 12 h, yield: 60 %.

conversion of 9-anthraceneacetic acid<sup>[18]</sup> to the vinamidine hexafluorophosphate salt under various reaction conditions failed,<sup>[19]</sup> presumably due to the sterically hindered 9-anthryl group.

Consequently, a “chemistry-on-the-complex” approach was attempted, in which a palladium-catalyzed cross-coupling was adopted to incorporate the bulky anthryl group into the [Ru(tpy)]<sup>2+</sup> moiety.<sup>[17]</sup> Treatment of complex **1b** with 9-anthryl boronic acid<sup>[16]</sup> under optimized Suzuki coupling reaction conditions afforded the monocoupling product, complex **2c**, which was purified by silica chromatography (Scheme 2). In surveying suitable catalysts and reaction conditions, reactions catalyzed by [Pd(PPh<sub>3</sub>)<sub>4</sub>] at 90 °C showed the best activity and selectivity for the monocoupling reaction, with 83 % yield after recovering starting complex **1b**. A slightly lower temperature and an optimized reaction time were preferred for control of the monocoupling reaction. Prerduced palladium catalyst, [Pd(PPh<sub>3</sub>)<sub>4</sub>], afforded a better yield than [PdCl<sub>2</sub>(PPh<sub>3</sub>)<sub>2</sub>], due to the inefficient transmetalation of the latter with bulky 9-anthrylboronic acid.

The syntheses of bimetallic Ru<sup>II</sup> species were achieved through palladium-catalyzed homocoupling reactions on the appropriate chlorides in the monometallic complexes, **2c** and **1a**, respectively. Treatment of complex **2c** with the



Scheme 2. Palladium-catalyzed reactions to form **2c** and **2d**: a) 9-anthrylboronic acid, [Pd(PPh<sub>3</sub>)<sub>4</sub>], K<sub>2</sub>CO<sub>3</sub>, DMF, 110 °C, 16 h, yield: 49 %; b) 1.0 equiv **2c**, 15 mol % [Pd(OAc)<sub>2</sub>], 30 mol % *t*Bu<sub>2</sub>P(biph), 2.0 equiv K<sub>2</sub>CO<sub>3</sub>, DMF, 110 °C, 24 h, yield: 49 %.

Pd(0) catalyst, generated in situ by the combination of [Pd(OAc)<sub>2</sub>] with 2-(di-*tert*-butylphosphino)biphenyl led to the homocoupled bimetallic complex **2d** (Scheme 2). Treatment of complex **1a** under the same homocoupling conditions yielded bimetallic complex **2e** (Scheme 1). Interestingly, the standard Ni-catalyzed reaction normally used to homocouple two fragments failed to generate **2d** and **2e** under a variety of conditions.<sup>[4]</sup>

**<sup>1</sup>H NMR spectroscopy:** All of the newly synthesized complexes **2a–e** were characterized by <sup>1</sup>H NMR spectroscopy. The <sup>1</sup>H NMR chemical-shift data for complexes **2a–e** and for complexes **1a–b** are given in the Supporting Information. Although there are more than 20 independent proton signals in the chemical-shift range of 7–10 ppm, all of the signals are well separated and assignable with the assistance of two-dimensional experiments, such as COSY or NOESY experiments (Supporting Information).

**X-ray crystallography:** The solid-state structures of complexes **2a** and **2b** were determined by X-ray crystallography. The ORTEP diagrams of the cations of complexes **2a** and **2b** as well as selected bond parameters are shown in Figures 1 and 2, respectively.

The bond lengths and bond angles are typical of [Ru(tpy)]<sup>2+</sup> moieties, in which the terpyridine ligands adopt a pseudooctahedral coordination geometry about the Ru<sup>II</sup>. The pyrimidine rings in the two complexes are nearly coplanar to the tpy moieties (angles between planes of 7.8° in **2a**, 4.0 and 12.4° in **2b**). The coplanar pyrimidyl rings serve to extend the electron delocalization, which is crucial to develop the bichromophoric behavior. The secondary chromophores, anthracenes, are almost perpendicular to the pm-tpy moieties (angles between planes of 75° in **2a**, 55 and 64° in **2b**), which diminishes conjugation, thereby allowing the subunits to maintain their independent properties in the complexes. The combination of the coplanar pyrimidyl ring and

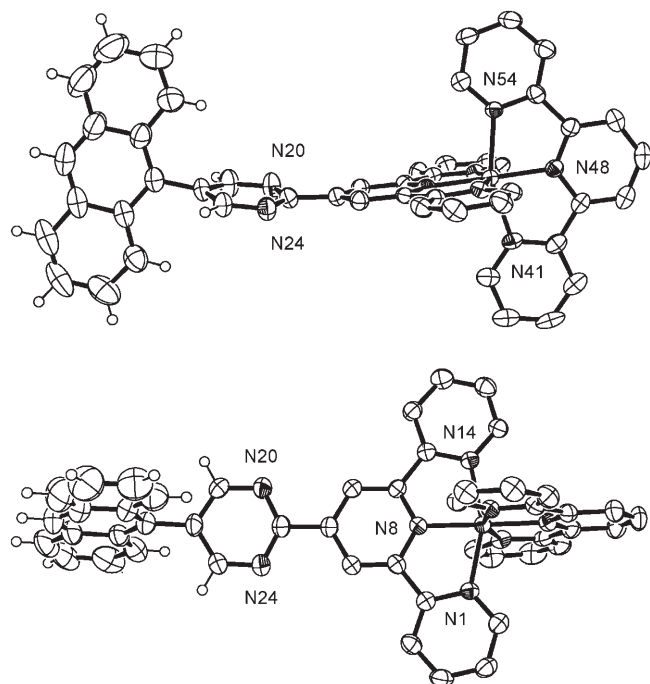


Figure 1. ORTEP plots of the X-ray crystal structure of complex **2a** exposing the tpy ligand (top) and, after a 90° rotation, the 4'-(5-(9-anthryl)-pyrimid-2-yl)-tpy ligand (bottom). Thermal ellipsoids are set at 50% probability with the counteranions, solvent and hydrogen atoms are omitted for clarity. Selected bond lengths (in Å) for **2a**: Ru–N1: 2.084(3); Ru–N8: 1.978(3); Ru–N14: 2.081(3); Ru–N41: 2.068(3); Ru–N48: 1.983(3); Ru–N54: 2.092(3).

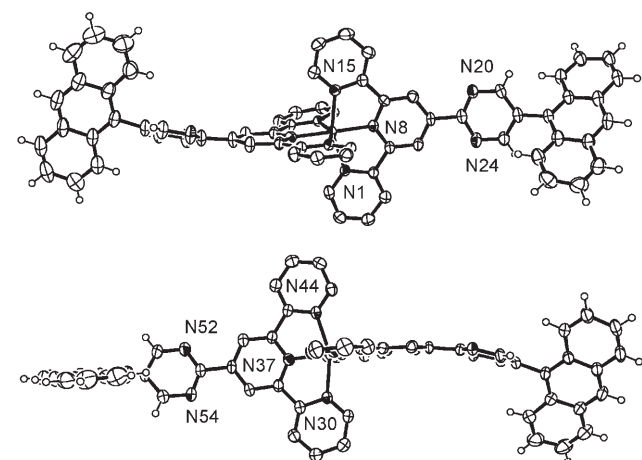


Figure 2. ORTEP plots of the X-ray crystal structure of complex **2b** exposing a 4'-(5-(9-anthryl)-pyrimid-2-yl)-tpy ligand (top) and, after a 90° rotation, the other 4'-(5-(9-anthryl)pyrimid-2-yl)-tpy ligand (bottom). Thermal ellipsoids are set at 50% probability with the counteranions, solvent and hydrogen atoms are omitted for clarity. Selected bond lengths (in Å) for **2b**: Ru–N1: 2.070(3); Ru–N8: 1.993(4); Ru–N15: 2.064(4); Ru–N30: 2.087(4); Ru–N37: 1.981(5); Ru–N44: 2.086(4).

perpendicular anthracene chromophore is crucial to the enhancement of the room-temperature luminescence lifetimes (see section on photophysical properties).

**Electrochemistry:** The electrochemical data for complexes **2a–e** are compiled in Table 1. In all the complexes, one quasi-reversible oxidation process is identified, which can be assigned easily to metal-centered oxidation. The anthracene-

Table 1. Electrochemical redox potentials for complexes **2a–e** and reference complex **3** in argon-purged acetonitrile.<sup>[a]</sup>

Compd	$E_{1/2ox}$ [V] ( $\Delta E_p$ [mV])	$E_{1/2red}$ [V] ( $\Delta E_p$ [mV])	
<b>2a</b>	1.32 (65)	–1.10 (65)	–1.40 (ir)
<b>2b</b>	1.36 (70)	–1.06 (70)	–1.30 (ir)
<b>2c</b>	1.35 (65)	–1.11 (84)	–1.32 (ir)
<b>2d</b>	1.34 (80) <sup>[b]</sup>	–1.05 (70)	–1.25 (ir)
<b>2e</b>	1.31 (70) <sup>[b]</sup>	–1.06 (70)	–1.25 (ir)
<b>3</b> <sup>[c]</sup>	1.30	–1.24	–1.49

[a] Scan rate 100 mV s<sup>–1</sup>.  $E_{1/2} = 1/2(E_{pa} + E_{pc})$ ;  $E_{pa}$  and  $E_{pc}$  are the anodic and cathodic peak potential, respectively.  $\Delta E_p = E_{pa} - E_{pc}$ . ir = irreversible. The reversible processes are mono-electronic, unless otherwise stated. Potentials are corrected by internal reference, ferrocene (395 mV). [b] Bi-electronic process. [c] **3** = [Ru(tpy)<sub>2</sub>]<sup>2+</sup>, from ref. [8m].

based oxidation process, which is known to occur around +1.40 V vs the saturated calomel electrode (SCE) and to be largely irreversible, does not occur up to +1.50 V, most likely because the metal oxidation processes displace the anthracene oxidation to more positive potentials. The oxidation processes of **2d** and **2e** are bielectronic, indicating that metal–metal electronic interaction across the bridging ligand is negligible from an electrochemical viewpoint. In all cases, the 4'-pyrimidine substituents on the tpy shifts metal oxidation(s) at slightly more positive potentials (by 25–50 mV) relative to the reference complex **3**, [Ru(tpy)<sub>2</sub>]<sup>2+</sup> (see Table 1), due to a slight stabilization of the metal-based orbitals by the electron-accepting pyrimidine substituents on the tpy ligands.

Heteroleptic complex **2a** is slightly easier to oxidize than homoleptic complex **2b**, which has two pyrimidine rings, as expected. Complex **2c** has an oxidation potential very close to that of **2b**, which suggests that the effect of the remote substituent on the pyrimidyl ring (chloride in **2c**, anthracene in **2b**) on metal oxidation is minimal. Similarly, the dimetallic complex **2d** also displays an oxidation potential close to those of **2b** and **2c**. Finally, complex **2e** has nearly the same oxidation potential as **2a**, and is definitely less positive than **2d**, due to the better electron-donating ability of the peripheral tpy ligands relative to the peripheral tpy-pm-an ligands that are present in **2d**.

As far as the reduction pattern is concerned, more than one reduction process can be observed with only the first process being reversible. Interestingly, the reduction processes of the newly synthesized complexes are shifted to less-negative potentials relative to [Ru(tpy)<sub>2</sub>]<sup>2+</sup>. For **2a**, the first one-electron reduction is assigned to the pyrimidyl-substituted ligand and the second one is attributed to the non-substituted tpy moiety. In **2b**, the first one-electron reduction, involving one of the identical pyrimidyl-substituted ligands, occurs at almost the same potential as the first reduction of **2a**, in agreement with the assignment of this latter

process. The slight difference in first reduction potential is due to the effect of the second ligand, with the nonsubstituted tpy ligand pushing more electron density onto the tpy-pm-an ligand by a secondary effect, which parallels the effect on metal-centered oxidation. The second reduction process of **2b** occurs at a less-negative potential than that of its heteroleptic counterpart **2a**, in agreement with the different electron-withdrawing abilities of the substituted and nonsubstituted tpy ligands. Compound **2c** also behaves similarly to **2a**, with the noticeable exception that its second reduction potential is less negative, in agreement with the electron-withdrawing ability of the pyrimidyl-chloride substituent.

The reduction pattern of **2d** warrants additional comments. In this compound, as well as in **2e**, a new bridging ligand is present, namely a tpy-pm-pm-tpy strand. For **2d**, it is not immediately obvious whether the first reduction involves the bridging ligand or one of the peripheral ligands. Although crystallographic data are not available for **2d** or **2e**, from the crystallographic data of **2a** and **2b** it can be proposed that each tpy-pm subunit is roughly planar, whereas the two halves of the large bridging ligand are not, because of steric hindrance between the hydrogen atoms of the two pyrimidine rings. Therefore, extended delocalization over the whole bridging ligand framework is prevented, although planarization is expected to increase upon reduction. The bridging ligand tpy-pm-pm-tpy can, therefore, be viewed as being made by two identical subunits, each one capable of being reduced at less-negative potentials than tpy. In any event, significant electronic interaction between the two halves of the bridge can be foreseen. In contrast, negligible interaction is expected between the two terminal tpy-pm-an ligands, on the basis of the negligible interaction between the metal centers, as evidenced by oxidation data (see above). As a consequence, whether or not the first reduction of **2d** should involve the peripheral ligands, such a process would probably be bielectronic. Because the first reduction of **2d** is mono-electronic, it is assigned to reduction of one of the two halves of the bridging ligand. The second reduction process of **2d** could be attributed to the peripheral ligands or to the second reduction of the bridge: to decide between these two options, comparison with the reduction potentials of **2e** is quite convenient. In fact, compound **2e** exhibits two reduction processes at very similar potentials to **2d**, and both of them are at less-negative potentials than the second tpy-based reduction in **3** and **2a**. As a consequence, both processes can be attributed to orbitals centered mainly on the bridging ligand. Following this attribution, the second reduction process of **2d** is, therefore, also attributed to bridging-ligand reduction. The potential difference between the first and second processes of both **2d** and **2e** (about 200 mV) could, therefore, be due to electron pairing within a large, delocalized orbital extending over the whole framework of the bridge or, if a localized situation would be considered, to electronic coupling between "isolated" sites (the two tpy-pm "halves"). Because reduction of aromatic systems, such as biphenyl or dimethylviologens,

strongly favors planarization and extended delocalization,<sup>[20]</sup> the electron pairing hypothesis is preferred for **2d** and **2e**.

**Absorption spectra:** The UV-visible spectra of **2a–e** are dominated by spin-allowed MLCT bands in the visible and by spin-allowed polypyridine ligand-centered (LC) bands in the UV region (Figure 3, Table 2). The spectra of complexes

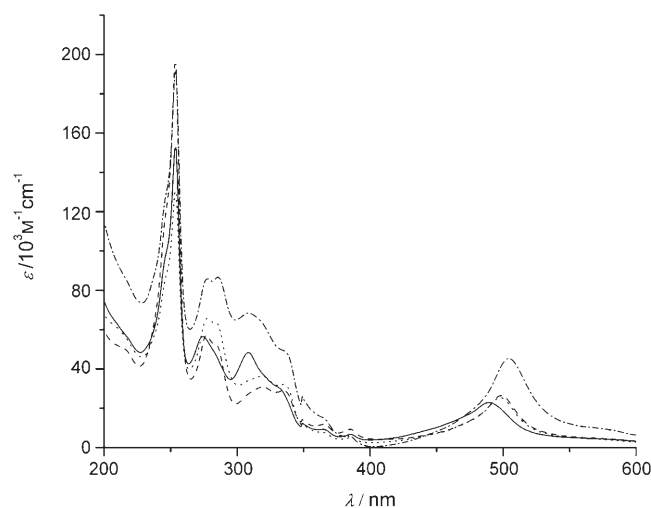


Figure 3. Electronic absorption spectra for **2a** (—), **2b** (---), **2c** (.....), **2d** (---), **2e** (-.-.-). The spectra were recorded in acetonitrile at RT.

Table 2. Electronic spectral data of complexes **2a–e** and [Ru(tpy)<sub>2</sub>]<sup>2+</sup> (**3**).<sup>[a]</sup>

Compd	$\lambda_{\max}$ [nm] ( $\epsilon$ [ $10^3 \text{ M}^{-1} \text{ cm}^{-1}$ ])
<b>2a</b>	489 (22.9); 308 (48.3); 274 (56.5); 254 (152.8)
<b>2b</b>	499 (39.6); 319 (46.3); 277 (85.8); 254 (292.6)
<b>2c</b>	498 (38.1); 319 (54.4); 278 (98.6); 254 (195.7)
<b>2d</b>	505 (65.7); 308 (99.2); 286 (125.7); 254 (278.5)
<b>2e</b>	497 (55.5); 308 (124.7); 273 (93.2)
<b>3</b> <sup>[b]</sup>	476 (10.4); 309 (46.2); 270 (28.1)

[a] Data were collected in deaerated, spectroscopic-quality acetonitrile at 298 K. [b] **3** = [Ru(tpy)<sub>2</sub>]<sup>2+</sup>, from reference [8m].

**2a–d** all have anthracene signatures in the 350–400 nm region, due to electronic transition to the <sup>1</sup>L<sub>a</sub> state, and at around 254 nm, due to electronic transition to the <sup>1</sup>B<sub>a</sub> state. As expected, the molar absorption of the anthracene-based bands in **2b** and **2d** are larger than those in **2a** and **2c**, respectively. Notably, the <sup>1</sup>MLCT bands of complexes **2a–e** are red-shifted (498–505 nm) relative to the prototypical [Ru(tpy)<sub>2</sub>]<sup>2+</sup> (474 nm) complex (Table 4). The lowering in energy of the MLCT absorption bands can be attributed mostly to the electron-withdrawing nature of the pyrimidine substituent (extended acceptor-orbital effect), also in agreement with redox data, because the 9-anthryl group has little electronic interaction with the tpy-pm moieties, due to its orthogonal arrangement. Notably, the lowest-energy absorption maxima of **2d** and **2e** are at slightly lower energy than those of **2a–c**, suggesting that the lowest-energy MLCT

Table 3. Luminescence data.

Compd	298 K <sup>[a]</sup>			77 K <sup>[b]</sup>	
	$\lambda_{\max}$ [nm]	$\tau$ [ns]	$\Phi$	$\lambda_{\max}$ [nm]	$\tau$ [ms]
<b>2a</b>	680	5.5; 402	$1.3 \times 10^{-4}$	692	3.5
<b>2b</b>	675	5.8; 1806	$1.8 \times 10^{-4}$	694	3.5
<b>2c</b>	678	18; 1300	$1.5 \times 10^{-4}$	692	3.6
<b>2d</b>	704	1040	$5.7 \times 10^{-4}$	695	5.3
<b>2e</b>	697	65	$5.0 \times 10^{-4}$	667	0.014

[a] In deaerated acetonitrile. [b] In butyronitrile.

transition in **2d** and **2e** involves the bridging ligand, in agreement with redox data.

### Photophysical properties

**Luminescence properties:** All the new complexes exhibit luminescence both at room temperature in fluid solution and at 77 K in rigid matrix (see Table 3, Figure 4).

Table 4. Population percentages at the equilibrium of anthracene-based (An) and MLCT triplets in the complexes studied, calculated by using thermodynamic and kinetic data.

Compound	$\Delta E$ <sup>[c]</sup>	Thermodynamics [%] <sup>[a]</sup>		Kinetics [%] <sup>[b]</sup>	
		MLCT	An	MLCT	An
<b>2a</b>	850	1.6	98.4	3.7	96.3
<b>2b</b>	970	0.9	99.1	1.2	98.8
<b>2c</b>	910	1.2	98.8	2.0	98.0
<b>2d</b>	470	10.0	90.0	2.0	98.0

[a] Calculated by using the Equation given in ref. [22]. [b] Calculated by using Equation (1), based on experimental data. [c]  $\Delta E$  = energy difference ( $\text{cm}^{-1}$ ) between MLCT and An triplets, estimated from data given in the text.

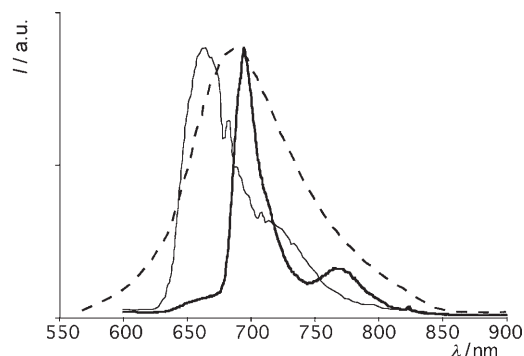


Figure 4. Luminescence spectra of **2d** in acetonitrile at RT (---) and of **2d** (— bold) and **2e** (— thin) in butyronitrile at 77 K.

The emission spectra and energies at room temperature are indicative of <sup>3</sup>MLCT emitters.<sup>[7,20]</sup> At low temperature, the <sup>3</sup>MLCT assignment is valid for **2e**, whereas the luminescence spectra and lifetimes suggest that the emission of **2a–d** is due to a triplet state of the anthracene moieties<sup>[11b]</sup> (in the case of **2d** a residual MLCT emission at about 650 nm is also visible at 77 K, see Figure 4, but its low intensity hampers lifetime measurement). This situation is actually very often observed in multichromophoric species made from a

metal complex and an aromatic hydrocarbon chromophore, if the low-lying, emitting MLCT state of the metallic subunit is close to the lowest-energy triplet of the organic chromophore.<sup>[11]</sup> Moreover, upon fitting particular thermodynamic and kinetic factors: 1) the lowest-energy level of the whole supermolecule is the organic triplet state, 2) the <sup>3</sup>MLCT state is accessible by Boltzmann distribution, and 3) the rate constants of interchromophoric energy-transfer processes highly exceed the intrinsic decays of the isolated subunits, and, of course, by assuming that the intrinsic decay of the organic triplet is several orders of magnitude slower than that of the metal-based excited state, as is usually the case,<sup>[11g]</sup> the room-temperature lifetimes of the multichromophoric species become biexponential, exhibiting a very short component, due to the prompt <sup>3</sup>MLCT emission, and a much longer-lived component, due to repopulation of the emitting <sup>3</sup>MLCT state from the lower-lying and intrinsically longer-lived organic triplet. In this case, the organic chromophores behave as excited-state energy-storage elements.<sup>[13]</sup> The situation is exemplified in Figure 5.

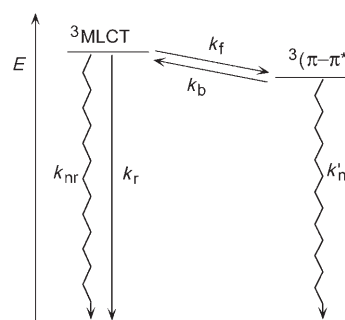


Figure 5. Schematic energy-level diagram and decay for complexes **2a–d**. <sup>3</sup>( $\pi$ - $\pi^*$ ) is the triplet anthracene state.  $k_f$  and  $k_b$  are the forward and back energy transfer, respectively, involved in the equilibration process. The equilibration rate constant  $k_{\text{eq}} = (k_f + k_b)$ .

The shorter lifetime takes into account the equilibration time between the initially formed MLCT state and the organic triplet level (it is, therefore, substantially shorter than the intrinsic lifetime of the isolated MLCT state), whereas the longer-lived component is the lifetime of the equilibrated state  $\tau_{\text{eq}}$ , in which the two relevant triplet states decay in concert.  $\tau_{\text{eq}}$  can be obtained by employing Equation (1):<sup>[11g]</sup>

$$\tau_{\text{eq}} = 1 / [(1-\alpha) \tau_{\text{MLCT}}^{-1} + \alpha \tau_{\text{ORG}}^{-1}] \quad (1)$$

Here,  $\tau_{\text{MLCT}}$  and  $\tau_{\text{ORG}}$  are the intrinsic lifetimes of the isolated metal-based and aromatic hydrocarbon chromophores, respectively, and  $\alpha$  and  $(1-\alpha)$  are the population percentages of the hydrocarbon-based and metal-based chromophore triplets at equilibrium, respectively.<sup>[11e,22]</sup>

For complexes **2a–d**, the energy of the anthracene triplet (<sup>3</sup>An) is assumed to be constant ( $14410 \text{ cm}^{-1}$ , from the 77 K emission of the **2a–d** compounds), and the energy level of the <sup>3</sup>MLCT state of the various complexes at room temperature can be estimated by room-temperature emission spectral-fitting parameters.<sup>[1k,7a]</sup> This latter procedure gives

15260 cm<sup>-1</sup> for **2a**, 15380 cm<sup>-1</sup> for **2b**, 15320 cm<sup>-1</sup> for **2c**, and 14880 cm<sup>-1</sup> for **2d** as the energy level of the relevant <sup>3</sup>MLCT states. As a consequence, it appears that for the various compounds, the excited-state equilibrium should shift smoothly towards anthracene triplet population along the series **2d**, **2a**, **2c**, and **2b**, if the only factor to consider was thermodynamics (namely, excited-states energy gap).

Indeed, luminescence lifetimes of the multichromophoric species **2a**, **2b**, and **2c** are biexponential, with a short component that can be assigned to the prompt MLCT emission, quenched with respect to suitable model species by the equilibration process, and a longer component that can be attributed to deactivation of the equilibrated state according to Equation (1). The intrinsic lifetimes of the MLCT excited state in the various species can be assumed to be close to those of reference models, which are (structural formulae are shown in Figure 6) [(tpy)Ru(tpy-pm-phenyl)]<sup>2+</sup> for **2a** (reference lifetime, 15 ns),<sup>[23]</sup> [(phenyl-pm-tpy)Ru(tpy-pm-phenyl)]<sup>2+</sup> for **2b** (reference lifetime, 21 ns),<sup>[24]</sup> [(Cl-pm-

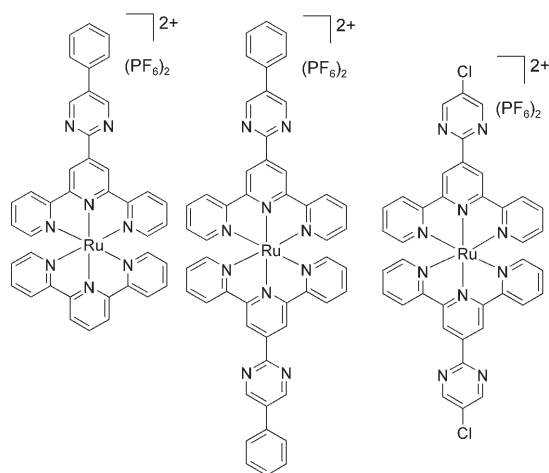


Figure 6. Model compounds for photophysical studies. From left, [(tpy)Ru(tpy-pm-phenyl)]<sup>2+</sup>,<sup>[23]</sup> [(phenyl-pm-tpy)Ru(tpy-pm-phenyl)]<sup>2+</sup>,<sup>[24]</sup> and **1b**.<sup>[24]</sup>

tpy)Ru(tpy-pm-Cl)]<sup>2+</sup> for **2c** (reference lifetime, 26 ns<sup>[24]</sup>). From these latter data, the rate constants of the equilibration process for **2a–c** can be approximated to  $1.1 \times 10^8$ ,  $1.0 \times 10^8$ , and  $1.7 \times 10^7$  s<sup>-1</sup>, respectively. Because absolute values of equilibration rate constants should be treated with care, and due to the experimental uncertainty regarding the luminescence lifetimes (conservative estimation; 10% for monoexponential decays, 20% for biexponential decays), it appears that the process is slower for **2c** than for **2a** and **2b**. Apart from any effect due to a difference in driving force (which is quite small within this series of complexes) for the forward and back energy-transfer processes determining the equilibration rate constants, we attribute such an observation to the nature of the MLCT state involved: in **2a** and **2b**, the acceptor ligand of the MLCT state is also the ligand carrying the anthracene chromophore, so the coupling between the two excited states involved in the equilibration process

should be quite large, whereas in **2c**, the acceptor ligand of the lowest-energy MLCT state involves the chloride-substituted ligand, and the coupling between this MLCT state and the anthracene-based triplet (centered on the other ligand) is expected to be lower.<sup>[25]</sup>

Both compounds **2d** and **2e** exhibit only a monoexponential luminescence decay. Although this was expected for **2e**, which does not contain the anthracene chromophore and shows a typical <sup>3</sup>MLCT excited-state lifetime, this was unexpected for **2d**, also on the basis of its emission lifetime, and is clearly due to the equilibrated state. In this case, the equilibration process is probably faster than the equipment resolution (2 ns). This circumstance is not in line with arguments based on thermodynamics (for **2d**, the driving force for the forward energy transfer from the MLCT state to the anthracene triplet should be the smallest in the multichromophoric species studied here) or on the nature of the MLCT involved (the acceptor ligand of the lowest-energy MLCT state in **2d** would be the bridging ligand, i.e., as for **2c**, not the one carrying the anthracene chromophore). We have no simple explanation for such behavior.

As mentioned above, the equilibrated-state lifetime should depend mainly on the partition between <sup>3</sup>MLCT and <sup>3</sup>An states. The intrinsic lifetime of the latter state should be constant in all compounds studied here and is assumed to be 350 μs (the reported lifetime of the anthracene triplet in a Ru<sup>II</sup> species, at room temperature in acetonitrile, obtained by transient absorption spectroscopy<sup>[27]</sup>), and the intrinsic lifetimes of **2a–d** are close to each other, ranging from 15 to 26 ns (see above). There are two simple methods to estimate the population percentage at the equilibrium of the <sup>3</sup>MLCT and <sup>3</sup>An states: one method is based on thermodynamic parameters, that is, the energies of the relevant excited states as reported above and application of the Boltzmann distribution,<sup>[22]</sup> and the other is based on experimental kinetic data. Table 4 lists the data obtained by the two different methods. A fair agreement between the two methods is found for **2a–c**, whereas for **2d**, the experimental equilibrated time (and consequently, the <sup>3</sup>An population calculated by the kinetic data) exceeds the value expected by thermodynamics. This somewhat puzzling behavior parallels the surprisingly fast equilibration time of **2d** discussed above. Apparently, the properties of **2d** seem to be governed by factors that have not yet been fully clarified.

*Transient absorption spectroscopy:* To characterize further the excited-state properties of the complexes, we performed nanosecond transient absorption spectroscopy in acetonitrile at room temperature. The differential absorption spectrum of each compound typically exhibits a bleach in the MLCT absorption region and a broad and weak absorption in the 550–700 nm region. Such differential changes agree well with the MLCT nature of the excited state, for which the broad absorption in the 550–700 nm region is attributed mainly to the absorption of the reduced ligand. Although such a transient spectrum decays monoexponentially for **2e**, for **2a–2c** it evolves quickly (i.e., within a few tens of nano-

seconds) to reveal a strong absorption in the 390–460 nm range, typical of the anthracene triplet state.<sup>[11,26,28]</sup> Once this new absorption is formed, the whole transient spectrum decays monoexponentially on a longer timescale (microsecond range). Interestingly, the 390–460 nm absorption is already present within the excitation impulse for **2d**, which shows only a monoexponential decay at all wavelengths.

The kinetic analyses of the differential spectra are in good agreement with the luminescence data: as an example, the analysis of the differential absorption of **2c** (excitation, 532 nm) at 420 nm (the anthracene triplet state) shows the formation of a transient absorption (risetime, 17 ns) that then decays on longer timescales (decay time, 1380 ns). If the analysis wavelength is set at 490 nm (the MLCT bleach), the transient spectrum shows a biphasic recovery, which parallels the data of luminescence lifetimes. Figure 7 shows the kinetic profile of the transient signal of **2c** at 420 nm and Table 5 lists the kinetic data for all the compounds, which are in good agreement with those obtained from luminescence decays (Table 3).

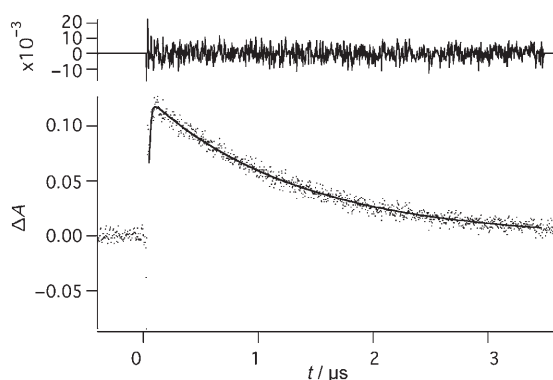


Figure 7. Kinetic profile of the transient absorption signal of **2c** in deaerated acetonitrile monitored at 420 nm. Excitation wavelength is 532 nm

Table 5. Kinetic data from transient absorption spectroscopy in deoxygenated acetonitrile at RT<sup>[a]</sup>. Excitation wavelength, 532 nm.

Compound	<b>2a</b>	<b>2b</b>	<b>2c</b>	<b>2d</b>	<b>2e</b>
$\tau$ [ns] ( $\lambda = 420$ nm)	5; 375	6; 1600	17; 1380	1060	<sup>[b]</sup>
$\tau$ [ns] ( $\lambda = 490$ nm)	5; 420	6; 1900	24; 1270	940 <sup>[c]</sup>	69

[a] Due to the intensity of the signals, the more reliable value for the shorter lifetime was obtained at 420 nm. [b] Signal too weak to be analyzed. [c]  $\lambda_{em} = 600$  nm.

## Conclusion

Three mononuclear and two dinuclear Ru<sup>II</sup> polypyridine complexes were synthesized and characterized by various methods, including X-ray crystallography, and their redox behavior, absorption spectra, luminescence properties (both at room temperature and at 77 K), and nanosecond transient absorption spectra and decays were studied.

The lowest-lying MLCT state of all the complexes involves a tpy-type species bearing a coplanar pyrimidine ring (tpy-pm ligand) as the acceptor ligand, so allowing extended

delocalization in the acceptor ligand of the MLCT state. Moreover, in most of the new compounds, secondary chromophores, namely anthracene subunits, were successfully incorporated into the tpy-pm framework through palladium-catalyzed Suzuki cross-coupling reactions, to gain multichromophore species. The fusion of two design strategies, the extended acceptor orbital and multichromophoric approaches, afforded long-lived luminescence in Ru<sup>II</sup> complexes at room temperature. Multiple luminescence lifetimes were obtained in most cases, as a consequence of fast equilibration between the promptly generated <sup>3</sup>MLCT emitting state and the close-lying triplet state of the anthryl moieties. Thermodynamic and kinetic factors governing the equilibration time and the lifetime of the equilibrated excited state confirm that the multichromophore approach is viable for generating long-lived excited states in Ru<sup>II</sup> complexes of tridentate ligands. Further work will consider long-range electron transfer in these new long-lived Ru<sup>II</sup> species.

## Experimental Section

**General:** All reactions were performed under a dry argon atmosphere by using standard Schlenk or glove-box techniques. All reactions involving anthracene were protected from laboratory light. Solvents were predried by using the Pure-Solv Solvent Purification System (Innovative Technology). Palladium catalysts and phosphine ligands were purchased from STREM. All other chemicals were purchased from Sigma-Aldrich and were used as received.

ESI-MS was performed by the Service de spectrométrie de masse at the Université de Montréal. Absorption and emission spectra were measured in deaerated acetonitrile at RT by using a Cary 500i UV-Vis-NIR spectrophotometer and a Cary Eclipse fluorescence spectrophotometer or a Jobin-Yvon Spex Fluoromax P (equipped with a Hamamatsu R3896 photomultiplier), respectively. Luminescence spectra were corrected for photomultiplier response by using a program purchased with the fluorimeter. Luminescence lifetimes were measured by using an Edinburgh OB 900 time-correlated single-photon counting spectrometer employing a Hamamatsu PLP2 laser diode as pulse (wavelength output, 408 nm; pulse width, 59 ps). Emission quantum yields were measured at RT by using the optically dilute method.<sup>[29]</sup> [Ru(bpy)<sub>3</sub>]<sup>2+</sup> in air-equilibrated aqueous solution was used as quantum yield standard ( $F = 0.028$ ).<sup>[30]</sup>

Nanosecond transient-absorption experiments were performed in argon-purged acetonitrile. A Continuum Surelite SLI-10 Nd:YAG laser was used to excite the sample with 10-ns pulses at 355 nm. The monitoring beam was supplied by a Xe arc lamp, and the signal was detected by a red-sensitive photodiode after being passed through a high-radiance monochromator. Differential absorption spectra were recorded point-by-point, whereas kinetic measurements were made at fixed wavelength. 64 individual laser shots were averaged to improve the reliability of each acquisition. The signals were stored and analyzed in a dedicated PC.

Electrochemistry data were collected in deaerated acetonitrile with 0.1 M Bu<sub>4</sub>NPF<sub>6</sub> by using a BAS CV-50W voltammetric analyzer. Redox potentials were corrected by the internal reference ferrocene (395 mV vs SCE).

Experimental uncertainties were as follows: absorption maxima,  $\pm 2$  nm; molar absorption coefficients, 10%; emission maxima,  $\pm 5$  nm; excited-state lifetimes, 10%; luminescence quantum yields, 20%; redox potentials,  $\pm 10$  mV.

**X-ray crystallography:** Recrystallization of **2a** and **2b** from acetonitrile by slow diffusion of diisopropylether provided single red crystals suitable for X-ray crystallography. CCDC299069 and 299070 contain the supplementary crystallographic data for this paper. These data can be obtained



free of charge from The Cambridge Crystallographic Data Centre via [www.ccdc.cam.ac.uk/data\\_request/cif](http://www.ccdc.cam.ac.uk/data_request/cif).

### Syntheses

Pyrimidyl tpy ligands were synthesized from terpyridylamine hydrochloride and vinamidium hexafluorophosphate salt.<sup>[19]</sup> Complexes **1a,b** were synthesized as reported previously.<sup>[10d]</sup> 9-Anthrylboronic acid was prepared by following the literature methods.<sup>[16]</sup>

**Complex 2a** [(*an-pm-tpy*)Ru(*tpy*)]/[PF<sub>6</sub>]<sub>2</sub>: Complex [(Cl-*pm-tpy*)Ru(*tpy*)]/[PF<sub>6</sub>]<sub>2</sub> (**1a**, 0.100 g, 0.10 mmol), 9-anthryl boronic acid (0.100 g, 0.46 mmol), [PdCl<sub>2</sub>(PPh<sub>3</sub>)<sub>2</sub>] (8.0 mg, 10 mol %), and K<sub>2</sub>CO<sub>3</sub> (0.140 g, 1.0 mmol) were added to anhydrous DMF (10 mL). The reaction mixture was heated to 110 °C for 12 h under argon. The mixture was then poured into deaerated aqueous NH<sub>4</sub>PF<sub>6</sub> and filtered through Celite. The residue was subjected to chromatography on silica gel with acetonitrile and aqueous saturated KNO<sub>3</sub> solution (7:1) as eluent. After anion exchange to hexafluorophosphate with NH<sub>4</sub>PF<sub>6</sub>, pure red product **2a** (0.095 g, 85 %) was isolated. <sup>1</sup>H NMR (500 MHz, CD<sub>3</sub>CN): δ = 9.86 (s, 2H; H<sub>3,5</sub>), 9.26 (s, 2H; H<sub>P3,5</sub>), 8.82 (s, 1H; H<sub>An10</sub>), 8.80 (d, *J* = 8.2 Hz, 2H; H<sub>T3,5</sub>), 8.76 (d, *J* = 8.1 Hz, 2H; H<sub>3,3'</sub>), 8.54 (d, *J* = 8.0 Hz, 2H; H<sub>T3,3'</sub>), 8.47 (t, *J* = 8.2 Hz, 1H; H<sub>T4</sub>), 8.25 (d, *J* = 8.5 Hz, 2H; H<sub>An4,5</sub>), 7.98 (td, *J* = 8.2 Hz, *dJ* = 1.2 Hz, 2H; H<sub>4,4'</sub>), 7.96 (td, *J* = 7.8 Hz, *dJ* = 1.3 Hz, 2H; H<sub>T4,4'</sub>), 7.82 (d, *J* = 8.8 Hz, 2H; H<sub>An1,8</sub>), 7.65 (m, 2H; H<sub>An3,6</sub>), 7.59 (m, 2H; H<sub>An2,7</sub>), 7.47 (d, *J* = 5.6 Hz, 2H; H<sub>6,6'</sub>), 7.42 (d, *J* = 4.9 Hz, 2H; H<sub>T6,6'</sub>), 7.23 (ddd, *J* = 7.4, 5.7, 1.1 Hz, 2H; H<sub>5,5'</sub>), 7.20 ppm (ddd, *J* = 7.5, 5.7, 1.1 Hz, 2H; H<sub>T5,5'</sub>); <sup>13</sup>C NMR (75 MHz, CD<sub>3</sub>CN): δ = 160.5, 159.9, 158.0, 158.0, 156.2, 155.2, 152.7, 152.6, 144.6, 138.3, 138.2, 136.3, 132.9, 131.4, 130.7, 128.9, 128.9, 128.3, 127.7, 127.6, 127.0, 125.9, 125.5, 124.9, 124.6, 123.9, 121.7 ppm (br); ESI-MS: *m/z*: 411.2 [M-2PF<sub>6</sub>]<sup>2+</sup>; elemental analysis calcd (%) for C<sub>48</sub>H<sub>32</sub>F<sub>12</sub>N<sub>6</sub>P<sub>2</sub>Ru·1.5H<sub>2</sub>O: C 50.62, H 3.10, N 9.84; found: C 50.78, H 2.73, N 9.56.

**Complex 2b** [Ru(*an-pm-tpy*)<sub>2</sub>]/[PF<sub>6</sub>]<sub>2</sub>: Complex [Ru(Cl-*pm-tpy*)<sub>2</sub>]/[PF<sub>6</sub>]<sub>2</sub> (**1b**, 0.080 g, 0.074 mmol), 9-anthryl boronic acid (0.090 g, 0.41 mmol), [PdCl<sub>2</sub>(PPh<sub>3</sub>)<sub>2</sub>] (11.0 mg, 20 mol %), and K<sub>2</sub>CO<sub>3</sub> (0.065 g, 0.47 mmol) were added to dry anhydrous DMF (10 mL). The mixture was heated at 140 °C for 12 h under argon and poured into deaerated aqueous NH<sub>4</sub>PF<sub>6</sub> and filtered through Celite. The residue was subjected to chromatography on silica gel with acetonitrile and aqueous saturated KNO<sub>3</sub> (10:1) solution as eluent. After anion exchange to hexafluorophosphate with NH<sub>4</sub>PF<sub>6</sub>, pure red product **2b** (0.061 g, 60 %) was isolated. <sup>1</sup>H NMR (500 MHz, CD<sub>3</sub>CN): δ = 9.92 (s, 4H; H<sub>3,5</sub>), 9.31 (s, 4H; H<sub>P4,6</sub>), 8.86 (s, 2H; H<sub>An10</sub>), 8.83 (d, *J* = 8.0 Hz, 4H; H<sub>3,3'</sub>), 8.29 (d, *J* = 8.4 Hz, 4H; H<sub>An4,5</sub>), 8.04 (td, *J* = 7.9 Hz, *dJ* = 1.3 Hz, 4H; H<sub>4,4'</sub>), 7.85 (d, *J* = 8.8 Hz, 4H; H<sub>An1,8</sub>), 7.68 (m, 4H; 2H; H<sub>An3,6</sub>), 7.62 (m, 4H; H<sub>An2,7</sub>), 7.57 (dd, *J* = 5.6, 0.6 Hz, 4H; H<sub>6,6'</sub>), 7.29 ppm (ddd, *J* = 7.5, 5.7, 1.2 Hz, 4H; H<sub>5,5'</sub>); <sup>13</sup>C NMR (75 MHz, CD<sub>3</sub>CN): δ = 160.5, 160.0, 158.0, 156.0, 152.8, 145.0, 138.4, 133.0, 131.4, 130.7, 128.9, 128.3, 127.8, 127.4, 127.4, 127.0, 125.9, 125.5, 125.1, 121.8 ppm; ESI/LR-MS: *m/z*: 1221.1 [M-PF<sub>6</sub>]<sup>+</sup>; 538.5 [M-2PF<sub>6</sub>]<sup>2+</sup>; elemental analysis calcd (%) for C<sub>66</sub>H<sub>42</sub>F<sub>12</sub>N<sub>10</sub>P<sub>2</sub>Ru·2H<sub>2</sub>O: C 56.54, H 3.31, N 9.99; found: C 56.66, H 3.15, N 10.17.

**Complex 2c** [(*an-pm-tpy*)Ru(*tpy-pm-Cl*)]/[PF<sub>6</sub>]<sub>2</sub>: Complex [Ru(Cl-*pm-tpy*)<sub>2</sub>]/[PF<sub>6</sub>]<sub>2</sub> (**1b**, 0.087 g, 0.080 mmol), 9-anthryl boronic acid (0.022 g, 0.099 mmol), [Pd(PPh<sub>3</sub>)<sub>4</sub>] (9.0 mg, 0.008 mmol, 10 mol %), and K<sub>2</sub>CO<sub>3</sub> (0.027 g, 0.20 mmol) were added to anhydrous DMF (10 mL). The mixture was heated at 90 °C for 24 h under argon and poured into deaerated aqueous NH<sub>4</sub>PF<sub>6</sub> and filtered through Celite. The residue was subjected to chromatography on silica gel with acetonitrile and aqueous saturated KNO<sub>3</sub> solution (15:1) as eluent. After anion exchange to hexafluorophosphate with NH<sub>4</sub>PF<sub>6</sub>, pure red product **2c** (0.039 g, 49 %, 83 % after recovery of starting material **1b**) was isolated. <sup>1</sup>H NMR (400 MHz, CD<sub>3</sub>CN): δ = 9.89 (s, 2H; H<sub>3,5</sub>), 9.68 (s, 2H; H<sub>T3,5</sub>), 9.27 (s, 2H; H<sub>A4,6</sub>), 9.18 (s, 2H; H<sub>B4,6</sub>), 8.83 (s, 1H; H<sub>An10</sub>), 8.79 (d, *J* = 8.0 Hz, 2H; H<sub>3,3'</sub>), 8.75 (d, *J* = 8.1 Hz, 2H; H<sub>T3,3'</sub>), 8.26 (d, *J* = 8.4 Hz, 2H; H<sub>An4,5</sub>), 8.00 (t, *J* = 7.9 Hz, 4H; H<sub>4,4'</sub>, H<sub>T4,4'</sub>), 7.82 (d, *J* = 8.4 Hz, 2H; H<sub>An1,8</sub>), 7.62 (m, 4H; H<sub>An2,3,6,7</sub>), 7.52 (d, *J* = 5.7 Hz, 2H; H<sub>6,6'</sub>), 7.48 (d, *J* = 5.6 Hz, 2H; H<sub>T6,6'</sub>), 7.25 (t, *J* = 7.6 Hz, 2H; H<sub>5,5'</sub>), 7.21 ppm (t, *J* = 7.5 Hz, 2H; H<sub>T5,5'</sub>); ESI-MS: *m/z*: 467.0 [M-2PF<sub>6</sub>]<sup>2+</sup>.

**Complex 2d** [(*an-pm-tpy*)Ru(*tpy-pm-pm-tpy*)Ru(*tpy-pm-an*)]/[PF<sub>6</sub>]<sub>4</sub>: Complex [(*an-pm-tpy*)Ru(*tpy-pm-Cl*)]/[PF<sub>6</sub>]<sub>2</sub> (**2c**) (42.4 mg, 0.031 mmol),

[Pd(OAc)<sub>2</sub>] (1.1 mg, 0.005 mmol, 15 mol %), *t*Bu<sub>2</sub>P(biphenyl) (2.9 mg, 0.010 mmol, 30 mol %), and K<sub>2</sub>CO<sub>3</sub> (18.5 mg, 0.13 mmol) were added to anhydrous DMF (10 mL). The mixture was heated at 110 °C for 24 h under argon and poured into deaerated aqueous NH<sub>4</sub>PF<sub>6</sub> and filtered through Celite. The residue was subjected to chromatography on silica gel with acetonitrile and aqueous saturated KNO<sub>3</sub> solution (7:1) as eluent. After anion exchange to hexafluorophosphate with NH<sub>4</sub>PF<sub>6</sub>, pure red product **2d** (12.5 mg, 49 %, 62 % after recovery of starting material **2c**) was isolated. <sup>1</sup>H NMR (400 MHz, CD<sub>3</sub>CN): δ = 9.93 (s, 4H; H<sub>3,5</sub>), 9.86 (s, 4H; H<sub>T3,5</sub>), 9.71 (s, 4H; H<sub>B4,6</sub>), 9.31 (s, 4H; H<sub>A4,6</sub>), 8.86 (s, 2H; H<sub>An10</sub>), 8.83 (dd, *J* = 8.2 Hz, 8H; H<sub>3,3'</sub>, H<sub>T3,3'</sub>), 8.29 (d, *J* = 8.8 Hz, 4H; H<sub>An4,5</sub>), 8.05 (dt, *J* = 8.5 Hz, 8H; H<sub>4,4'</sub>, H<sub>T4,4'</sub>), 7.85 (d, *J* = 8.4 Hz, 4H; H<sub>An1,8</sub>), 7.65 (m, 8H; H<sub>An2,3,6,7</sub>), 7.58 (d, *J* = 5.6 Hz, 4H; H<sub>6,6'</sub>), 7.54 (d, *J* = 5.7 Hz, 4H; H<sub>T6,6'</sub>), 7.29 ppm (dt, *J* = 6.7 Hz, 8H; H<sub>5,5'</sub>, H<sub>T5,5'</sub>); <sup>13</sup>C NMR: insufficient solubility in CD<sub>3</sub>CN; ESI-MS: *m/z*: 450.2 [M-4PF<sub>6</sub>]<sup>4+</sup>; 648.2 [M-3PF<sub>6</sub>]<sup>3+</sup>; 1045.0 [M-2PF<sub>6</sub>]<sup>2+</sup>.

**Complex 2e** [(*tpy*)Ru(*tpy-pm-pm-tpy*)Ru(*tpy*)]/[PF<sub>6</sub>]<sub>4</sub>: Complex [(*tpy*-Ru(*tpy-pm-Cl*)]/[PF<sub>6</sub>]<sub>2</sub> (**1a**) (31.1 mg, 0.032 mmol), [Pd(OAc)<sub>2</sub>] (1.1 mg, 0.005 mmol, 15 mol %), *t*Bu<sub>2</sub>P(biphenyl) (2.9 mg, 0.010 mmol, 30 mol %), and K<sub>2</sub>CO<sub>3</sub> (11.0 mg, 0.80 mmol) were added into anhydrous DMF (5 mL). The mixture was heated at 110 °C for 24 h under argon and poured into deaerated aqueous NH<sub>4</sub>PF<sub>6</sub> and filtered through Celite. The residue was subjected to chromatography on silica gel with 7:1 CH<sub>3</sub>CN and aqueous saturated KNO<sub>3</sub> solution as eluent. After anion exchange to hexafluorophosphate with NH<sub>4</sub>PF<sub>6</sub>, pure red product **2e** (22.5 mg, 0.012 mmol, 75 %) was isolated. <sup>1</sup>H NMR (500 MHz, CD<sub>3</sub>CN) δ = 9.79 (s, 4H; H<sub>T3,5</sub>), 9.66 (s, 4H; H<sub>Pm4,6</sub>), 8.80 (d, *J* = 8.2 Hz, 4H; H<sub>3,5</sub>), 8.76 (d, *J* = 8.0 Hz, 4H; H<sub>T3,3'</sub>), 8.53 (d, *J* = 8.2 Hz, 4H; H<sub>3,3'</sub>), 8.47 (t, *J* = 8.2 Hz, 2H; H<sub>4</sub>), 8.00 (td, *J* = 7.8 Hz, *dJ* = 1.4 Hz, 4H; H<sub>T4,4'</sub>), 7.95 (td, *J* = 7.8 Hz, *dJ* = 1.3 Hz, 2H; H<sub>4,4'</sub>), 7.44 (d, *J* = 5.5 Hz, 4H; H<sub>6,6'</sub>), 7.41 (d, *J* = 5.7 Hz, 4H; H<sub>T6,6'</sub>), 7.24 (ddd, *J* = 7.5, 5.5, 1.1 Hz, 4H; H<sub>T5,5'</sub>), 7.15 ppm (ddd, *J* = 7.5, 5.7, 1.1 Hz, 4H; H<sub>5,5'</sub>); <sup>13</sup>C NMR insufficient solubility in CD<sub>3</sub>CN; ESI-MS: *m/z*: 322.0 [M-4PF<sub>6</sub>]<sup>4+</sup>; 478.4 [M-3PF<sub>6</sub>]<sup>3+</sup>; 789.6 [M-2PF<sub>6</sub>]<sup>2+</sup>.

### Acknowledgements

Financial support by the NSERC (Canada), Université de Montréal, Università di Messina, Università di Bologna (Funds for selected topics), and FIRB (Project no. RBNE019H9K) are gratefully acknowledged. Francine Bélanger-Gariépy is thanked for help with the X-ray crystallography. Johnson-Matthey is thanked for a loan of precious metals.

- [1] This topic is too vast to be quoted exhaustively. For representative contributions, see: a) V. Balzani, F. Scandola, *Supramolecular Photochemistry*, Horwood, Chichester, **1991**; b) G. L. Closs, J. R. Miller, *Science* **1988**, *240*, 440; c) M. R. Wasielewski, *Chem. Rev.* **1992**, *92*, 435; d) K. D. Jordan, M. N. Paddon-Row, *Chem. Rev.* **1992**, *92*, 395; e) V. Balzani, L. De Cola, *Supramolecular Chemistry*, Kluwer, Dordrecht, **1992**; f) D. Gust, T. A. Moore, A. L. Moore, *Acc. Chem. Res.* **1993**, *26*, 198, and references therein; g) K. P. Ghiggino, T. A. Smith, *Prog. React. Kinet.* **1993**, *18*, 375; h) R. A. Bissel, A. P. de Silva, H. Q. N. Gunaratne, P. L. M. Lynch, G. E. M. Maguire, C. P. McCoy, K. R. A. S. Sandanayake, *Top. Curr. Chem.* **1993**, *168*, 223; i) V. Balzani, A. Juris, M. Venturi, S. Campagna, S. Serroni, *Chem. Rev.* **1996**, *96*, 759, and references therein; j) L. Hammarström, F. Barigelletti, L. Flamigni, M. T. Indelli, N. Armaroli, G. Calogero, M. Guardigli, A. Sour, J.-P. Collin, J.-P. Sauvage, *J. Phys. Chem. A* **1997**, *101*, 9061; k) V. Balzani, A. Credi, M. Venturi, *Molecular Devices and Machines*, Wiley-VCH, Weinheim, **2003**; l) J. H. Alstrum-Acevedo, M. K. Brennaman, T. J. Meyer, *Inorg. Chem.* **2005**, *44*, 6802, and references therein; m) S. Welter, F. Lafalet, E. Cecchetto, F. Vergeer, L. De Cola, *ChemPhysChem* **2005**, *6*, 2417; n) M. N. Paddon-Row in *Electron Transfer in Chemistry* (Ed.: V. Balzani), VCH-Wiley, **2001**, Vol. 3, p. 180; o) D. Gust, T. A. Moore, A. L. Moore in *Electron Transfer in Chemistry* (Ed.: V. Balzani), VCH-Wiley, **2001**,

- Vol. 3, p. 272, and references therein; p) F. Scandola, C. Chiorboli, M. T. Indelli, M. A. Rampi in *Electron Transfer in Chemistry* (Ed.: V. Balzani), VCH-Wiley, **2001**, Vol. 3, p. 337, and references therein; q) V. Balzani, M. Clemente-Léon, A. Credi, B. Ferrer, M. Venturi, A. H. Flood, J. F. Stoddart, *Proc. Natl. Acad. Sci. USA* **2006**, *103*, 1178.
- [2] a) S. Serroni, G. Denti, S. Campagna, A. Juris, M. Ciano, V. Balzani, *Angew. Chem.* **1992**, *104*, 1540; *Angew. Chem. Int. Ed. Engl.* **1992**, *31*, 1493; b) S. Campagna, G. Denti, S. Serroni, A. Juris, M. Venturi, M. V. Ricevuto, *Chem. Eur. J.* **1995**, *1*, 211.
- [3] V. Balzani, S. Campagna, G. Denti, A. Juris, S. Serroni, M. Venturi, *Acc. Chem. Res.* **1998**, *31*, 26.
- [4] K. O. Johansson, J. A. Lotoski, C. C. Tong, G. S. Hanan, *Chem. Commun.* **2000**, 819.
- [5] Y.-Q. Fang, M. I. J. Polson, G. S. Hanan, *Inorg. Chem.* **2003**, *42*, 5.
- [6] F. Loiseau, R. Passalacqua, S. Campagna, M. I. J. Polson, Y.-Q. Fang, G. S. Hanan, *Photochem. Photobiol. Sci.* **2002**, *1*, 982.
- [7] a) T. J. Meyer, *Pure Appl. Chem.* **1986**, *58*, 1193; b) A. Juris, V. Balzani, F. Barigelletti, S. Campagna, P. Belser, A. von Zelewsky, *Coord. Chem. Rev.* **1988**, *84*, 85; c) K. Kalyanasundaram, *Photochemistry of Polypyridine and Porphyrin Complexes*, Academic Press, London, **1991**; d) V. Balzani, F. Barigelletti, L. De Cola, *Top. Curr. Chem.* **1990**, *158*, 31; e) G. J. Karvanos, N. J. Turro, *Photoinduced Electron Transfer*, VCH, New York, **1993**.
- [8] a) E. C. Constable, *Prog. Inorg. Chem.* **1994**, *42*, 67; b) E. M. Kober, J. L. Marshall, W. J. Dressick, B. P. Sullivan, J. V. Caspar, T. J. Meyer, *Inorg. Chem.* **1985**, *24*, 2755; c) C. R. Hecker, A. K. I. Gushurst, D. R. McMillin, *Inorg. Chem.* **1991**, *30*, 538; d) E. Amouyal, M. Mouallem-Bahout, G. Calzaferri, *J. Phys. Chem.* **1991**, *95*, 7641; e) C. R. Arana, H. D. Abruña, *Inorg. Chem.* **1993**, *32*, 194; f) J.-P. Collin, S. Guillerez, J.-P. Sauvage, F. Barigelletti, L. De Cola, L. Flamigni, V. Balzani, *Inorg. Chem.* **1992**, *31*, 4112; h) V. Grossshenny, R. Ziessel, *J. Chem. Soc. Dalton Trans.* **1993**, 817; i) V. Grossshenny, R. Ziessel, *J. Organomet. Chem.* **1993**, *453*, C19; j) A. Harriman, R. Ziessel, *Chem. Commun.* **1996**, 1707; k) F. Barigelletti, L. Flamigni, V. Balzani, J.-P. Collin, J.-P. Sauvage, A. Sour, E. C. Constable, A. M. W. Cargill Thompson, *J. Chem. Soc. Chem. Commun.* **1993**, 942; l) F. Barigelletti, L. Flamigni, V. Balzani, J.-P. Collin, J.-P. Sauvage, A. Sour, E. C. Constable, A. M. W. Cargill Thompson, *J. Am. Chem. Soc.* **1994**, *116*, 7692; m) F. Barigelletti, L. Flamigni, V. Balzani, J.-P. Collin, J.-P. Sauvage, A. Sour, *New J. Chem.* **1995**, *19*, 793; n) J.-P. Sauvage, J.-P. Collin, J.-C. Chambron, S. Guillerez, C. Coudret, V. Balzani, F. Barigelletti, L. De Cola, L. Flamigni, *Chem. Rev.* **1994**, *94*, 993; o) S. U. Son, K. H. Park, Y.-S. Lee, B. Y. Kim, C. H. Choi, M. S. Lah, Y. H. Jang, D.-J. Jang, Y. K. Chung, *Inorg. Chem.* **2004**, *43*, 6896; p) M. Maestri, N. Armaroli, V. Balzani, E. C. Constable, A. M. W. Cargill Thompson, *Inorg. Chem.* **1995**, *34*, 2759; q) J. Wang, Y.-Q. Fang, G. S. Hanan, F. Loiseau, S. Campagna, *Inorg. Chem.* **2005**, *44*, 5; r) E. A. Medlycott, G. S. Hanan, *Chem. Soc. Rev.* **2005**, *34*, 133.
- [9] M. I. J. Polson, E. A. Medlycott, G. S. Hanan, L. Mikelsons, N. J. Taylor, M. Watanabe, Y. Tanaka, F. Loiseau, R. Passalacqua, S. Campagna, *Chem. Eur. J.* **2004**, *10*, 3640.
- [10] a) A. El-ghayoury, A. Harriman, A. Khatyr, R. Ziessel, *Angew. Chem.* **2000**, *112*, 191; *Angew. Chem. Int. Ed.* **2000**, *39*, 185; b) A. C. Benniston, A. Harriman, V. Grossshenny, R. Ziessel, *New J. Chem.* **1997**, *21*, 405; c) A. El-ghayoury, A. Harriman, A. Khatyr, R. Ziessel, *J. Phys. Chem. A* **2000**, *104*, 1512; d) Y.-Q. Fang, N. J. Taylor, G. S. Hanan, F. Loiseau, R. Passalacqua, S. Campagna, H. Nieren-garten, A. Van Dorsselaer, *J. Am. Chem. Soc.* **2002**, *124*, 7912.
- [11] a) W. E. Ford, M. A. J. Rodgers, *J. Phys. Chem.* **1992**, *96*, 2917; b) G. J. Wilson, A. Launikonis, W. H. F. Sasse, A. W.-H. Mau, *J. Phys. Chem. A* **1997**, *101*, 4860; c) J. A. Simon, S. L. Curry, R. H. Schmehl, T. R. Schatz, P. Piotrowiak, X. Jin, R. P. Thummel, *J. Am. Chem. Soc.* **1997**, *119*, 11012; d) D. S. Tyson, C. R. Luman, X. Zhou, F. N. Castellano, *Inorg. Chem.* **2001**, *40*, 4063; e) B. Maubert, N. D. McClenaghan, M. T. Indelli, S. Campagna, *J. Phys. Chem. A* **2003**, *107*, 447; f) J. Wang, G. S. Hanan, F. Loiseau, S. Campagna, *Chem. Commun.* **2004**, 2068; g) N. D. McClenaghan, B. Maubert, M. T. Indelli, S. Campagna, *Coord. Chem. Rev.* **2005**, *249*, 1336; h) X. Y. Wang, A. Del Guerso, R. H. Schmehl, *J. Photochem. Photobiol. C* **2004**, *5*, 55; i) S. Leroy-Lhez, C. Belin, A. D'Aleo, R. Williams, L. De Cola, F. Fages, *Supramol. Chem.* **2003**, *15*, 627.
- [12] a) S. L. Murov, I. Carmichael, G. L. Hug, in *Handbook of Photochemistry*, Marcel Dekker, New York, **1993**; b) *Handbook of Photochemistry*, 3rd ed. (Eds.: M. Montalti, A. Credi, L. Prodi, M. T. Gandolfi), CRC Press, **2006**.
- [13] R. Passalacqua, F. Loiseau, S. Campagna, Y.-Q. Fang, G. S. Hanan, *Angew. Chem.* **2003**, *xx*, xxxx; *Angew. Chem. Int. Ed.* **2003**, *42*, 1608.
- [14] V. Farina, V. Krishnamurthy, W. J. Scott, *The Stille Reaction*, Wiley, New York, **1998**.
- [15] The same inductive effect was observed in the 4'-position of tpy ligands in Ru<sup>II</sup> complex: E. C. Constable, A. M. W. C. Thompson, D. A. Tocher, M. A. M. Daniels, *New J. Chem.* **1992**, *16*, 855.
- [16] Z. H. Li, M. S. Wong, Y. Tao, M. D'Iorio, *J. Org. Chem.* **2004**, *69*, 921.
- [17] a) N. Miyaoura, T. Yanagi, A. Suzuki, *Synth. Commun.* **1981**, *11*, 513; b) A. Suzuki, *Pure Appl. Chem.* **1985**, *57*, 1749; c) A. Suzuki, *Pure Appl. Chem.* **1991**, *63*, 419; d) A. R. Martin, Y. Yang, *Acta Chem. Scand.* **1993**, *47*, 221; e) A. Suzuki, *Pure Appl. Chem.* **1994**, *66*, 213; f) N. Miyaoura, A. Suzuki, *Chem. Rev.* **1995**, *95*, 2457; g) S. P. Stanforth, *Tetrahedron* **1998**, *54*, 263; h) N. Miyaoura, *Adv. Met.-Org. Chem.* **1998**, *6*, 187; i) A. J. Suzuki, *Organomet. Chem.* **1999**, *576*, 147; j) "Organoboranes for Syntheses" A. Suzuki, *ACS Symp. Ser.* **2001**, *783*, 80.
- [18] a) E. J. Ciganek, *Org. Chem.* **1980**, *45*, 1497; b) R. A. Gardner, J.-G. Delcros, F. Konate, F. Breitbeil III, B. Martin, M. Sigman, M. Huang, O. Phanstiel IV, *J. Med. Chem.* **2004**, *47*, 6055.
- [19] I. W. Davies, J.-F. Marcoux, J. Wu, M. Palucki, E. G. Corley, M. A. Robbins, N. Tsou, R. G. Ball, P. Dormer, R. D. Larsen, P. J. Reider, *J. Org. Chem.* **2000**, *65*, 4571.
- [20] a) A. Almenningen, O. Bastiansen, L. Fernholt, B. N. Cyvin, S. J. Cyvin, S. Samdal, *J. Mol. Struct.* **1985**, *128*, 59; b) K. Furuya, H. Torii, Y. Furukawa, M. Tasumi, *Theochem* **1998**, *424*, 225.
- [21] G. A. Crosby, *Acc. Chem. Res.*, **1975**, *8*, 231.
- [22] The Boltzmann distribution is expressed by the general formula:  $\frac{n_i}{N} = \frac{g_i e^{-E_i/k_B T}}{q}$  in which  $g_i$  is the degeneracy of the  $i$  level,  $E_i$  is the energy difference between the states,  $k_B$  is the Boltzmann constant, and  $q$  is the molecular partition function, taken as:  $q = \sum g_i e^{-E_i/k_B T}$  (only the first two terms in the summation expressing  $q$  are considered).
- [23] Y.-Q. Fang, N. J. Taylor, G. S. Hanan, F. Loiseau, R. Passalacqua, S. Campagna, H. Nieren-garten, A. Van Dorsselaer, *J. Am. Chem. Soc.* **2002**, *124*, 7912.
- [24] F. Loiseau et al., unpublished data.
- [25] Concerning the rate of energy transfer from MLCT triplets to appended anthracene triplet, a recent paper reports subpicosecond timescales (ref. [26]). However, in this case the driving force of the process is much larger ( $>2000 \text{ cm}^{-1}$ ) than in our systems—in fact, no equilibration between the triplet states is gained—and the linkage is flexible, allowing optimization of electronic factors.
- [26] J. R. Schoonover, D. M. Dattelbaum, A. Malko, V. I. Klimov, T. J. Meyer, D. J. Styers-Barnett, E. Z. Gannon, J. C. Granger, W. S. Aldridge, J. M. Papanikolas, *J. Phys. Chem. A* **2005**, *109*, 2472.
- [27] D. S. Tyson, K. B. Henbest, J. Bialecki, F. N. Castellano, *J. Phys. Chem. A* **2001**, *105*, 8154.
- [28] A. Credi, V. Balzani, S. Campagna, G. S. Hanan, C. R. Arana, J.-M. Lehn, *Chem. Phys. Lett.* **1995**, *243*, 105, and references therein.
- [29] J. N. Demas, G. A. Crosby, *J. Phys. Chem.* **1971**, *75*, 991.
- [30] N. Nakamaru, *Bull. Chem. Soc. Jpn.* **1982**, *55*, 2697.

Received: February 21, 2006  
Published online: August 22, 2006